Article:

ARTICLE

Ultrasmall, Ultracompact and Ultrahigh Efficient InGaN Micro Light Emitting Diodes (µLEDs) with Narrow Spectral Line Width

Jie Bai, Yuefei Cai, Peng Feng, Peter Fletcher, Chenqi Zhu, Ye Tian, and Tao Wang*

Cite This: https://dx.doi.org/10.1021/acsnano.0c01180

Read Online

ACCESS | Metrics & More | Article Recommendations | Supporting Information

ABSTRACT: Augmented reality and visual reality (AR and VR) microdisplays require micro light emitting diodes (µLEDs) with an ultrasmall dimension (≤ 5 µm), high external quantum efficiency (EQE), and narrow spectral line width. Unfortunately, dry etching which is the most crucial step for the fabrication of µLEDs in current approaches introduces severe damages, which seem to become an insurmountable challenge for achieving ultrasmall µLEDs with high EQE. Furthermore, it is well-known that µLEDs which require InGaN layers as an emitting region naturally exhibit significantly broad spectral line width, which becomes increasingly severe toward long wavelengths such as green. In this paper, we have reported a combination of our selective overgrowth approach developed very recently and epitaxial lattice-matched distributed Bragg reflectors (DBRs) embedded in order to address all these fundamental issues. As a result, our µLEDs with a diameter of 3.6 µm and an interpitch of 2 µm exhibit an ultrahigh EQE of 9% at ~500 nm. More importantly, the spectral line width of our µLEDs has been significantly reduced down to 25 nm, the narrowest value reported so far for III-nitride green µLEDs.

KEYWORDS: µLEDs, selective overgrowth, InGaN/GaN, distributed Bragg reflector, external quantum efficiency, dry-etching
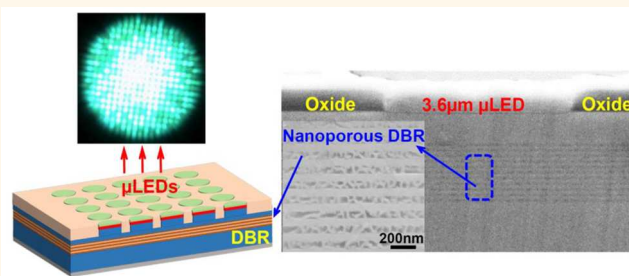
There is a significant growing interest in developing III-nitride microLEDs (µLEDs), the key components for microdisplays which are crucial for smart phones, smart watches, and augmented reality and visual reality (AR and VR) devices.[1−5] These kinds of devices are typically utilized in small spaces or at close proximity to the eye, and it therefore requests that µLEDs exhibit high resolution and high luminance. This is particularly important for AR/VR microdisplays which require µLEDs with an ultrasmall diameter (≤ 5 µm), high external quantum efficiency (EQE), and narrow spectral line width.

Currently, a standard photolithography technique combined with subsequent dry-etching processes remains a typical approach to the fabrication of µLEDs, in particular µLEDs with a small diameter (≤ 50 µm).[6−11] Consequently, this approach unavoidably introduces severe damage induced during dry-etching and follow-up processes, significantly enhancing nonradiative recombination and thus severely degrading the optical performance.[12−17] This issue becomes increasingly severe with decreasing the dimension of µLEDs.[13,14,18,19] Dry-etching processes also deteriorate the shape of µLEDs, ultimately affecting the resolution of microdisplay. As a result, the EQE of the µLED with a diameter of ≤ 5 µm is limited to a few percent, which does not meet practical requirements at all.[3,19,20]

More importantly, a significant reduction in the spectral line width of µLEDs is required in order to achieve microdisplays with high resolution especially for AR and VR. This tends to be extremely challenging, as it is well-known that InGaN LEDs exhibit an intrinsically broad spectral line width mainly as a result of indium segregation and alloy fluctuation, which becomes more severe with increasing emission wavelength (where higher indium composition is required, further enhancing both indium segregation and alloy fluctuation and thus making spectral line width even broader).

In order to overcome the limitations, it is necessary to develop a different approach or process, which allows us to not only further increase the EQE of µLEDs (especially for

ultrasmall μLEDs) but also significantly reduce their spectral line width. In this paper, we will demonstrate a different approach to achieving the two objectives simultaneously.

Very recently, we have reported a fundamentally different method, demonstrating ultrasmall and ultracompact green μLEDs with a diameter of 3.6 μm and an interpitch of 2 μm.[21] The μLEDs exhibit an EQE of 6% at 515 nm and a nice shape compared with the current state-of-the-art.[21] The key to the success of our approach is due to the utilization of a direct epitaxial growth on a prepatterned template, which does not involve any dry-etching process that is the most crucial step in the conventional approaches mentioned above and thus eliminates any resultant etching damages. However, we must say that a further enhancement in EQE is still required for high performance microdisplays. Furthermore, the intrinsically broad spectral line width of μLEDs will have to be significantly reduced.

A promising approach to meeting the objectives simultaneously is to introduce a reflector below the emitting region of μLEDs (i.e., an InGaN/GaN multiple quantum well (MQW) region). It would be ideal to epitaxially integrate μLEDs and distributed Bragg reflectors (DBRs) with a high reflectivity, as this can not only further enhance light extraction efficiency but also potentially reduce the spectral line width of μLEDs.

Lattice-mismatched AlGaN/GaN or AlN/GaN DBRs have been[22−25] widely studied but suffer from a number of severe issues, such as cracking and rough surface caused as a result of strain accumulation.[26] Furthermore, the intrinsically small contrast in refractive index between AlN and GaN requires a large number of pairs (typically, 30−40 pairs) in order to achieve a high reflectivity, thus costing substantial epitaxial growth time which is not particularly appealing for industry.

Lattice-matched DBRs with a significantly high contrast in refractive index between two alternating layers in each pair are ideal, leading to a decrease in the number of pairs requested and thus a reduction in epitaxial growth time. This also naturally maintains the high crystal quality of GaN for the growth of any further device structures. Very recently, nanoporous (NP) GaN has been intensively studied for the fabrication of lattice-matched DBRs by means of electrochemical (EC) etching.[27−29] For the details about the fabrication of the nanoporous DBRs, please refer to Methods.

RESULTS AND DISCUSSION

Figure 1 shows the reflectance spectra of a few lattice-matched DBR reflectors as examples. In each case, 11 pairs of NP-GaN/undoped GaN are used, and these DBR reflectors cover a wide spectrum from blue to amber by simply tuning the thicknesses of n++-type GaN and undoped GaN in each pair. The three DBR reflectors all exhibit a high reflectivity of >96% and a broad stopband. In detail, the stopband is ~85 nm for blue, ~115 nm for green/yellow, and 134 nm for amber. As an example, the inset shows the typical cross-sectional scanning electron microscopy (SEM) image of the NP-GaN/undoped GaN DBRs for blue taken under a high magnification, where the alternating NP-GaN and undoped GaN can be clearly observed.

Our strategy is to combine the lattice-matched DBRs and our selective overgrowth method[20] which we have reported very recently, aiming to achieve μLEDs with a further increased EQE and significantly reduced spectra line width. Figure 2a schematically illustrates our invention incorporating such bottom DBRs.
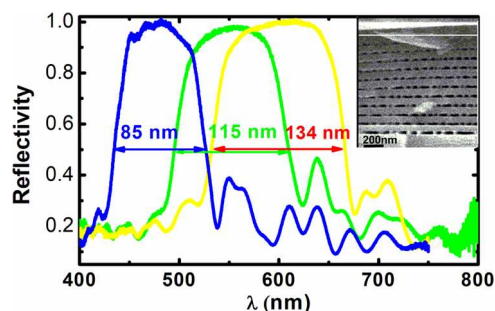

Figure 1. Reflectance spectra of three lattice-matched DBR reflectors, demonstrating these DBRs exhibit a high reflectivity of >96% and a broad stopband in a wide spectral region from blue to amber. Inset: Typical cross-sectional SEM image of the NP-GaN/undoped GaN DBRs for blue, where the alternating NP-GaN and undoped GaN can be clearly observed.
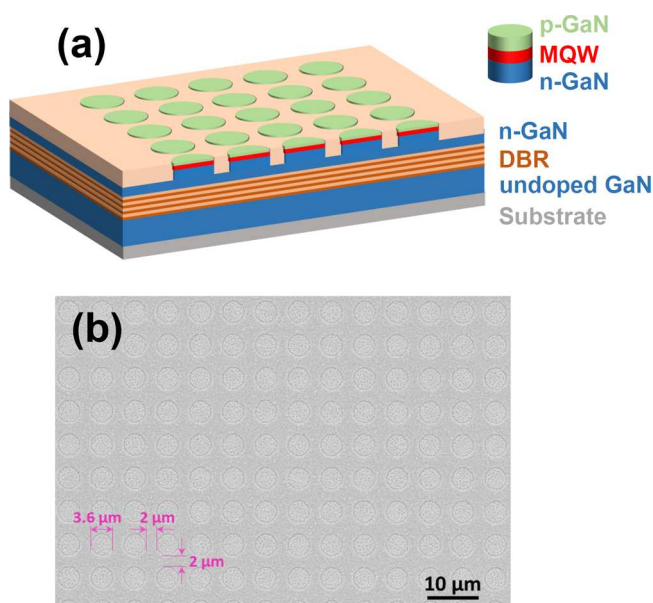

Figure 2. (a) Schematic of our invention for our μLED arrays incorporating with DBRs underneath. (b) Plan view SEM image of our regularly arrayed μLED wafer showing a diameter of 3.6 μm and an interpitch of 2 μm.

A standard n-type GaN layer (with a doping level of ~5 × 10^18/cm^3) with a thickness of 600 nm is further grown on the above epiwafer which contains 11 pairs of alternating n++-type GaN and undoped GaN. This is used as a template for further SiO2 microhole array patterning on its top. For the details about the patterning processes, please refer to our paper published very recently.[21] Basically, a SiO2 film with a thickness of 500 nm is initially deposited on the template by means of employing a standard plasma-enhanced chemical vapor deposition (PECVD) technique. Afterward, standard photolithography and drying etching techniques are used to selectively etch the dielectric layer down to the n-type GaN surface, forming regularly arrayed microholes with a diameter of 3.6 μm and an interpitch of 2 μm as we did previously.

Next, a standard InGaN-based LED structure is selectively grown on such a patterned template by a standard metal-organic vapor phase epitaxy (MOVPE) technique. The growth of the LED structure starts with an n-type GaN layer and then an InGaN prelayer (5% indium content), followed by five
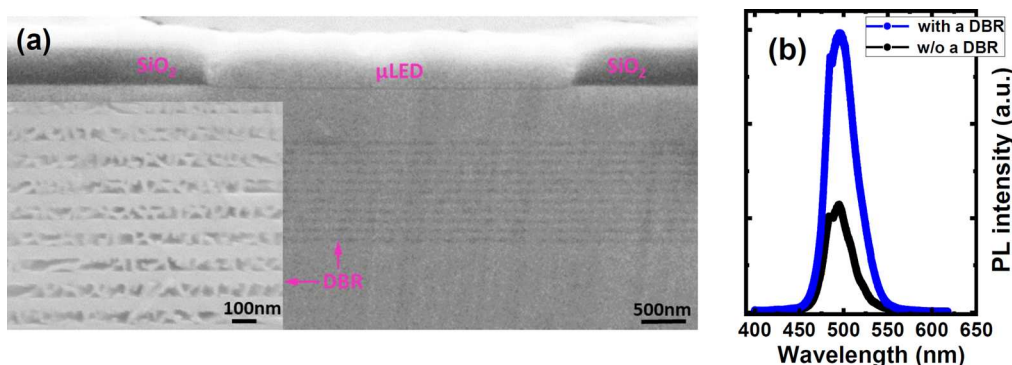
Figure 3. (a) Cross-sectional SEM image of our μLEDs with DBRs containing 11 pairs of NP-GaN/u-GaN formed after EC etching. Inset shows the cross-sectional SEM image of the DBRs taken under a high magnification. (b) PL spectra of both the μLED samples with and without a DBR reflector measured under identical conditions at room temperature.

periods of InGaN/GaN MQWs (2.5 nm InGaN quantum well; 13.5 nm GaN barrier) as an active region and then a 20 nm p-type $Al_{0.2}Ga_{0.8}N$ acting as a blocking layer on which a 200 nm p-type GaN is finally grown. The total thickness of the overgrown layers is ~500 nm, which is similar to that of the SiO_2 masks. Because of the dielectric masks, the growth of the LED structure is restricted within the microholes, leading to the natural formation of μLED arrays. All the physical parameters, such as the diameter, the individual location, the shape, and the interpitch, are fully determined by the SiO_2 microhole masks, meaning that the formation of μLED arrays does not involve any μLED mesa etching processes. Therefore, the dimension, the individual location, the shape, and the interpitch of μLEDs are under full control.

Figure 2b shows the typical SEM image of our regularly arrayed μLED eipi-wafer, demonstrating a nice circular shape and a very high uniformity in terms of shape, diameter, and interpitch. The diameter of each μLED is 3.6 μm and the interpitch is only 2 μm, which are similar to those grown on SiO_2 microhole arrays on a standard single n-type GaN layer (i.e., not on a template containing any pairs of alternating n^{++}-type GaN and undoped GaN).[21] Once again, it is important to highlight that such μLED arrays are fully compatible with any current microdisplay technique, such as the pick-and-place method widely used[13] or direct integration with transistor arrays which offer active-matrix switching for individually addressable μLED-based microdisplays.[31]

Subsequently, the standard EC processes described above have been carried out on part of the regularly arrayed μLED epiwafer in order to form DBRs underneath as a first step for device fabrication. The rest of the epiwafer which is called the "as-grown sample" is used for comparison. The EC processes have been conducted in 0.5 M nitric acid at 8 V bias using the μLED wafer as an anode and a Pt plate as a cathode. It is worth highlighting the doping level of the n^{++}-type GaN layer in each pair is more than 1 order of magnitude higher than that of the n-type GaN layer above the DBR region, which ensures that the n^{++}-type GaN layers in each pair of DBRs converts into NP-GaN while the n-type GaN layer remains intact during the EC etching.

Figure 3a displays the cross-sectional SEM image of our μLED epiwafer after the EC etching. The inset provides the cross-sectional SEM image taken under a high magnification, clearly indicating 11 pairs of NP-GaN/undoped GaN layers which form DBRs with a center wavelength at ~500 nm as designed.

Figure 3b shows the photoluminescence (PL) spectra of an as-grown μLED sample (without EC etching, that is, without DBRs below the InGaN/GaN MQWs) and the sample after EC-etching (namely, with DBRs below the InGaN/GaN MQWs), both measured under identical conditions using a standard PL system (please refer to Methods).

Figure 3b demonstrates that the PL intensity of the μLEDs with the DBRs is significantly enhanced by a factor of 150% in comparison with the as-grown μLEDs (i.e., without DBRs), demonstrating a significantly enhanced extraction efficiency due to DBRs.

In order to demonstrate that the μLED samples with DBRs can be used for the fabrication of regularly arrayed μLEDs featuring ultrasmall dimension, ultrahigh efficiency, and ultrahigh resolution, we have simply fabricated it into a regularly arrayed μLED device with a standard area of 330 × 330 μm^2, which contains a few thousand of 3.6 μm μLED arrays connected, as schematically shown in Figure 4a. For a direct comparison, the μLED samples without EC etching (i.e., without DBRs) are also processed in the same batch. For the details of device fabrication, please refer to Methods.

In order to clearly demonstrate emitting μLED pixels, our micro-electroluminescence (EL) measurement system has been employed to record microscopy images, which are taken under a low injection current density. Our micro-EL system is equipped with two objective lenses (one with 10× magnification and NA = 0.28 and another one with 50× magnification and NA = 0.43).

Figure 4b,c shows two emission images of the μLEDs with DBRs at a low current density of 15 A/cm² taken under a low and a high magnification, respectively. Figure 4b shows a whole μLED array device with very bright emission, while Figure 3c clearly demonstrates μLED pixels. Note that this current density used for our μLEDs under operation is smaller than a standard current density (i.e., 22 A/cm² typically used for standard broad area LEDs). This implies that a microdisplay, if fabricated using our μLEDs, should have at least as a long lifetime as those of standard broad area LEDs, while the lifetime of a standard broad area LED is expected to exceed 100 000 h under normal operation conditions.[31]

Figure 5a,b displays the EL spectra of the μLEDs without DBRs and the μLEDs with DBRs measured as a function of injection current from 5 to 100 mA in a continuous wave (CW) mode at room temperature, that is, the current density from 15 to 300 A/cm². Both the μLED devices exhibit a single emission centered at ~500 nm and that the EL intensity
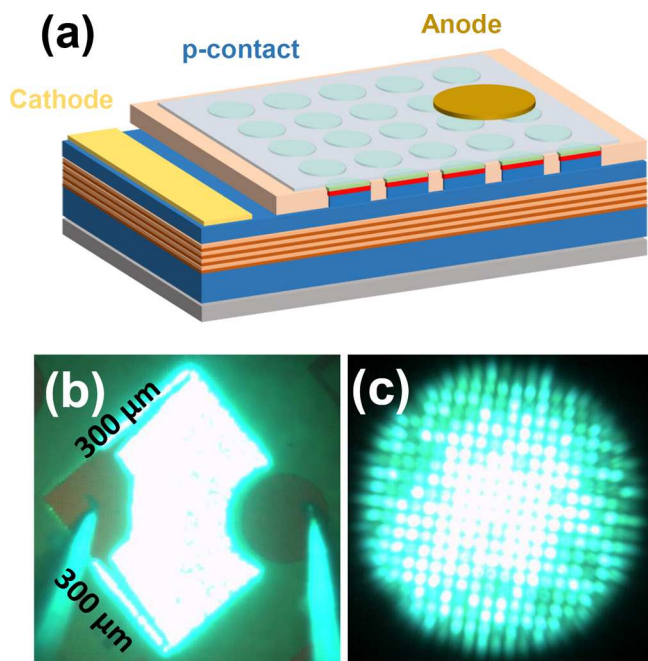
Figure 4. Schematic drawing of our µLED arrays (a). Emission microscopy images of our µLED arrays at an injection current density of 15 A/cm² under a low magnification (b) and under a high magnification (c).

increases continuously with increasing injection current density. However, it can be observed that there exists a clear difference between them in terms of spectra line width, that is, full width at half-maximum (fwhm).

Figure 5c shows the fwhm's of the EL spectra for both devices as a function of injection current, demonstrating that the µLEDs with DBRs show a significant reduction in the fwhm's of EL spectra in comparison with those of the µLEDs without DBRs as expected. In detail, at 20 mA injection current, the spectral line width (i.e., fwhm) drops from 31 nm

for the µLEDs without DBRs down to 25 nm for the µLEDs with DBRs, and it further drops from 37 to 29 nm at 100 mA. In addition, both samples show that the fwhm broadens with increasing injection current density due to the band-filling effect, which is often observed.[32]

Figure 5d shows the EL wavelengths of the µLEDs with and without DBRs as a function of injection current, both displaying a blue-shift in peak wavelength with increasing injection current, and the fingerprint of quantum-confined Stark effect (QCSE) generated as a result of strain-induced piezoelectric fields across the InGaN/GaN MQWs.[33,34] It is worth noting that the blue-shift (∼3.4 nm) for the µLEDs with DBRs is much smaller than that (∼8.7 nm) for the µLEDs without DBRs. This suggests that the strain-induced piezoelectric effect in the InGaN/GaN MQWs as an active region is slightly reduced due to partial strain release caused by forming the nanoporous DBRs underneath.

A LCS-100 characterization system is used to measure both light outputs and EQE on our bare-chip LEDs in a CW mode, where the system is equipped with an integrating sphere system and a CCD APRAR spectrometer.

Figure 6 exhibits the light output power of both devices (i.e., with and without DBRs) as a function of injection current density, demonstrating that the µLEDs with DBRs exhibit much higher light output than those without DBRs. For example, at a current density of 33 A/cm², the light output of the µLEDs with DBRs is 2.0 mW, while the light output of the µLEDs without DBRs is 1.2 mW, meaning 67% enhancement in light output is due to the utilization of DBRs.

Figure 6 also shows that the EQE of both devices as a function of current density. For both devices, the EQE increases initially with increasing current density and then reduces with further increasing current density as expected. However, for the µLEDs with DBRs the peak EQE is ∼9% at a current density of 33 A/cm², while the peak EQE of the µLEDs without DBRs is ∼6% which is similar to what we have reported very recently.[21] This is 50% higher for the µLEDs without DBRs than that for the µLEDs without DBRs.
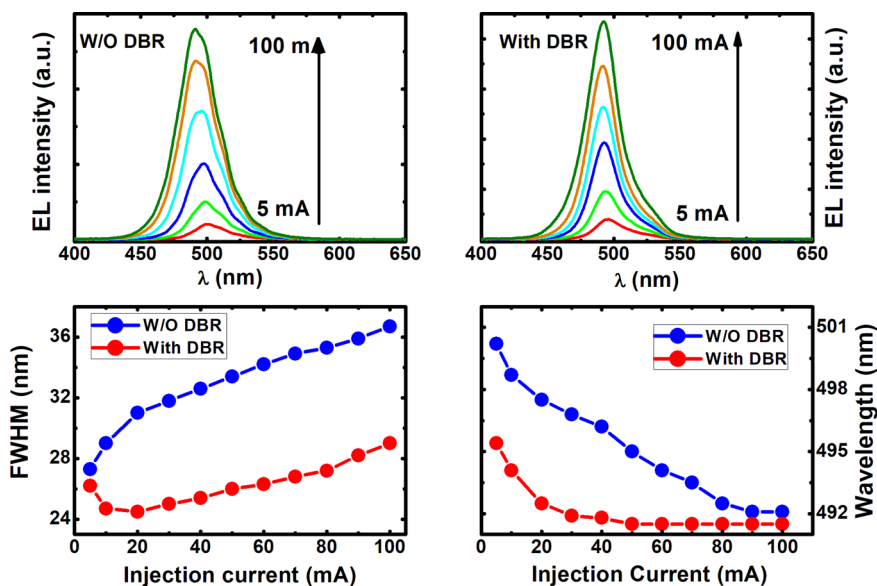

Figure 5. EL spectra of the µLED arrays without (a) and with DBRs (b), both measured as a function of injection current at room temperature. (c) The fwhm of EL spectra for both devices as a function of injection current. (d) Emission peak wavelength of both devices as a function of injection current.
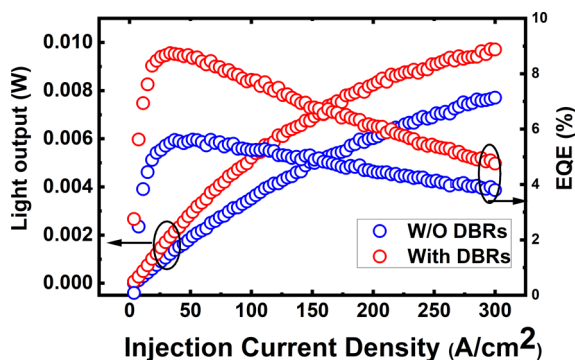
Figure 6. Light output and EQE of the μLED arrays with and without DBRs measured as a function of injection current density. Note that the measurements have been performed on a bare chip without any package or coating.

Furthermore, this EQE has been benchmarked against other reports for the ultrasmall μLEDs (i.e., with a diameter of ≤ 5 μm).[3,19,20] For details, please refer to Table S1 in Supporting Information.

CONCLUSIONS

In summary, we have reported a combination of our selective overgrowth approach and epitaxial lattice-matched DBRs embedded in order to address these fundamental and also challenging issues (ultrasmall dimension, high EQE, and narrow spectra line width) for achieving ultrasmall, high-efficiency, and high-resolution μLEDs. As a result, our μLEDs (i.e., with DBRs) with a diameter down to 3.6 μm and an interpitch down to 2 μm exhibit an ultrahigh maximum EQE of around 9%, which is 50% higher than those of the μLEDs without DBRs. More importantly, the spectral line width has been significantly reduced down to 25 nm, which is the narrowest value reported so far for III-nitride green μLEDs.

METHODS

Nanoporous DBR Growth. An epiwafer is first grown on a c-plane sapphire substrate by using a standard MOVPE technique. In detail, a 25 nm low-temperature GaN nucleation layer is grown after initial high-temperature annealing on a sapphire substrate, followed by the growth of a 1 μm GaN buffer layer at a high temperature, and then 11 pairs of alternating heavily silicon-doped n^{++}-type GaN (a doping level on an order of $>5 \times 10^{19}/cm^3$) and undoped GaN layers. Once the epiwafer is ready, a standard EC process is subsequently performed under bias in an acid electrolyte. The mechanism of EC etching is due to an initial oxidation process and a subsequent dissolution process in acidic solution under an anodic bias.[30] The injected holes oxidize GaN in an acidic electrolyte, where the oxidized layer is chemically dissolved and NP-GaN is then formed. Therefore, EC etching can be conducted only on highly conductive GaN (meaning that heavily silicon-doped n^{++}-type GaN is required), while undoped GaN or even n-type GaN (as long as the doping level is not that heavy) remains intact. Consequently, the pairs of n^{++}-type GaN/undoped GaN are converted into the pairs of NP-GaN/undoped GaN. Because of a significant contrast in refractive index between NP-GaN and undoped GaN, lattice-matched DBRs are formed.

Photoluminescence (PL) Measurements. PL measurements are performed by using a standard PL system equipped with a 375 nm diode laser as an excitation source, where a monochromator (Horiba SPEX 500M) is used to disperse the emission from a sample, and an air-cooled charge-coupled device is used to detect the emission.

Device Fabrication. As usual, indium-tin-oxide, which is deposited and then annealed in air at 600 °C for 1 min, is used as transparent p-type contact, while Ti/Al/Ni/Au alloys are used as n-

type contact. Both p-type and n-type electrodes are Ti/Au alloys. All the characteristics of our μLED chips in the present study are performed on bare chips, that is, no coating, no passivation, no epoxy, and no reflector, which are normally used for enhancing extraction efficiency. Current–voltage ($I-V$) characteristics of our μLED arrays with DBRs can be found in Supporting Information.

ASSOCIATED CONTENT

Ⓢ Supporting Information

The Supporting Information is available free of charge at https://pubs.acs.org/doi/10.1021/acsnano.0c01180.

> Additional material includes current–voltage characteristics of our μLEDs and the benchmark against the current state-of-the-art μLEDs with a dimension ≤ 5 μm (PDF)

AUTHOR INFORMATION

Corresponding Author

Tao Wang − *Department of Electronic and Electrical Engineering, University of Sheffield, Sheffield S1 3JD, United Kingdom;* ⓘ orcid.org/0000-0001-5976-4994; Email: t.wang@sheffield.ac.uk

Authors

Jie Bai − *Department of Electronic and Electrical Engineering, University of Sheffield, Sheffield S1 3JD, United Kingdom;* ⓘ orcid.org/0000-0002-6953-4698

Yuefei Cai − *Department of Electronic and Electrical Engineering, University of Sheffield, Sheffield S1 3JD, United Kingdom;* ⓘ orcid.org/0000-0002-2004-0881

Peng Feng − *Department of Electronic and Electrical Engineering, University of Sheffield, Sheffield S1 3JD, United Kingdom*

Peter Fletcher − *Department of Electronic and Electrical Engineering, University of Sheffield, Sheffield S1 3JD, United Kingdom*

Chenqi Zhu − *Department of Electronic and Electrical Engineering, University of Sheffield, Sheffield S1 3JD, United Kingdom*

Ye Tian − *Department of Electronic and Electrical Engineering, University of Sheffield, Sheffield S1 3JD, United Kingdom*

Complete contact information is available at:
https://pubs.acs.org/10.1021/acsnano.0c01180

Author Contributions

T.W. conceived the idea and organized the project. T.W. and J.B. prepared the manuscript. J.B. performed device fabrication and device characterization. Y.C., P. Feng, and C.Z. grew samples. P. Fletcher performed material characterization. Y.T. contributed to initial DBR fabrication.

Notes

The authors declare no competing financial interest.

REFERENCES

(1) Fan, Z. Y.; Lin, J. Y.; Jiang, H. X. III-Nitride Micro-Emitter Arrays: Development and Applications. *J. Phys. D: Appl. Phys.* **2008**, *41*, No. 094001.

(2) Han, H.-V.; Lin, H.-Y.; Lin, C.-C.; Chong, W.-C.; Li, J.-R.; Chen, K.-J.; Yu, P.; Chen, Te. M.; Chen, H.-M.; Lau, K.-M.; Kuo, H.-C. Resonant-Enhanced Full-Color Emission of Quantum-Dot-Based Micro LED Display Technology. *Opt. Express* 2015, 23, 32504.

(3) Templier, F. GaN-Based Emissive Microdisplays: A Very Promising Technology for Compact, Ultra-High Brightness Display Systems. *J. Soc. Inf. Disp.* 2016, 24, 669−675.

(4) Green, R. P.; McKendry, J. J. D.; Massoubre, D.; Gu, E.; Dawson, M. D.; Kelly, A. E. Modulation Bandwidth Studies of Recombination Processes in Blue and Green InGaN Quantum Well Micro-Light-Emitting Diodes. *Appl. Phys. Lett.* 2013, 102, No. 091103.

(5) Rajbhandari, S.; McKendry, J. J. D.; Herrnsdorf, J.; Chun, H.; Faulkner, G.; Haas, H.; Watson, I. M.; O'Brien, D.; Dawson, M. D. A Review of Gallium Nitride LEDs for Multi-Gigabit-Per-Second Visible Light Data Communications. *Semicond. Sci. Technol.* 2017, 32, No. 023001.

(6) Ozden, I.; Diagne, M.; Nurmikko, A. V.; Han, J.; Takeuchi, T. A Matrix Addressable 1024 Element Blue Light Emitting InGaN QW Diode Array. *Phys. Status Solidi A* 2001, 188, 139−142.

(7) Zhao, J. L.; Ka, M. W.; Chi, W. K.; Chak, W. T.; Kei, M. L. Monolithic LED Microdisplay on Active Matrix Substrate Using Flip-Chip Technology. *IEEE J. Sel. Top. Quantum Electron.* 2009, 15, 1298−1302.

(8) Otto, I.; Mounir, C.; Nirschl, A.; Pfeuffer, A.; Schapers, T.; Schwarz, U. T.; von Malm, N. Micro-Pixel Light Emitting Diodes: Impact of the Chip Process on Microscopic Electro- and Photo-luminescence. *Appl. Phys. Lett.* 2015, 106, 151108.

(9) Li, K. H.; Cheung, Y. F.; Tang, C. W.; Zhao, C.; Lau, K. M.; Choi, H. W. Optical Crosstalk Analysis of Micro-Pixelated GaN-Based Light-Emitting Diodes on Sapphire and Si Substrates. *Phys. Status Solidi A* 2016, 213, 1193−1198.

(10) Li, K. H.; Cheung, Y. F.; Cheung, W. S.; Choi, H. W. Confocal Microscopic Analysis of Optical Crosstalk in GaN Micro-Pixel Light-Emitting Diodes. *Appl. Phys. Lett.* 2015, 107, 171103.

(11) Lobo Ploch, N.; Rodriguez, H.; Stolmacker, C.; Hoppe, M.; Lapeyrade, M.; Stellmach, J.; Mehnke, F.; Wernicke, T.; Knauer, A.; Kueller, V.; Weyers, M.; Einfeldt, S.; Kneissl, M. Effective Thermal Management in Ultraviolet Light-Emitting Diodes with Micro-LED Arrays. *IEEE Trans. Electron Devices* 2013, 60, 782−786.

(12) Olivier, F.; Daami, A.; Licitra, C.; Templier, F. Influence of Size-Reduction on the Performances of GaN-Based Micro-LEDs for Display Application. *Appl. Phys. Lett.* 2017, 111, No. 022104.

(13) Wong, M. S.; Hwang, D.; Alhassan, A. I.; Lee, C.; Ley, R.; Nakamura, S.; DenBaars, S. P. High Efficiency of III-Nitride Micro-Light Emitting Diodes by Sidewall Passivation Using Atomic Layer Deposition. *Opt. Express* 2018, 26, 21324.

(14) Konoplev, S. S.; Bulashevich, K. A.; Karpov, S. Y. From Large-Size to Micro-LEDs: Scaling Trends Revealed by Modelling. *Phys. Status Solidi A* 2018, 215, 1700508.

(15) Yang, C.-M.; Kim, D.-S.; Park, Y. S.; Lee, J.-H.; Lee, Y. S.; Lee, J.-H. Enhancement in Light Extraction Efficiency of GaN-Based Light-Emitting Diodes Using Double Dielectric Surface Passivation. *Opt. Photonics J.* 2012, 02, 185−192.

(16) Zhang, Y.; Guo, E.; Li, Z.; Wei, T.; Li, J.; Ye, X.; Wang, G. Light Extraction Efficiency Improvement by Curved GaN Sidewalls in InGaN-Based Light-Emitting Diodes. *IEEE Photonics Technol. Lett.* 2012, 24, 243−245.

(17) Zuo, P.; Zhao, B.; Yan, S.; Yue, G.; Yang, H.; Li, Y.; Wu, H.; Jiang, Y.; Jia, H.; Zhou, J.; Chen, H. Improved Optical and Electrical Performances of GaN- Based Light Emitting Diodes with Nano Truncated Cone. *Opt. Quantum Electron.* 2016, 48, 1.

(18) Hwang, D.; Mughal, A.; Pynn, C. D.; Nakamura, S.; DenBaars, S. P. Sustained High External Quantum Efficiency in Ultrasmall Blue III-Nitride Micro-LEDs. *Appl. Phys. Express* 2017, 10, No. 032101.

(19) Templier, F.; Benaïssa, L.; Aventurier, B.; Nardo, C. D.; Charles, M.; Daami, A.; Henry, F.; Dupré, L. A Novel Process for Fabricating High-Resolution and Very Small Pixel-Pitch GaN LED Microdisplays. *Dig. Tech. Pap. - Soc. Inf. Disp. Int. Symp.* 2017, 48, 268−271.

(20) Smith, J. M.; Ley, R.; Wong, M. S.; Baek, Y. H.; Kang, J. H.; Kim, C. H.; Gordon, M. J.; Nakamura, S.; Speck, J. S.; DenBaars, S. P. Comparison of Size-Dependent Characteristics of Blue and Green InGaN MicroLEDs Down to 1 μm in Diameter. *Appl. Phys. Lett.* 2020, 116, No. 071102.

(21) Bai, J.; Cai, Y.; Feng, P.; Fletcher, P.; Zhao, X.; Zhu, C.; Wang, T. A Direct Epitaxial Approach to Achieving Ultrasmall and Ultrabright InGaN Micro Light-Emitting Diodes. *ACS Photonics* 2020, 7, 411−415.

(22) Nakada, N.; Nakaji, M.; Ishikawa, H.; Egawa, T.; Umeno, M.; Jimbo, T. Improved Characteristics of InGaN Multiple-Quantum-Well Light-Emitting Diode by GaN/AlGaN Distributed Bragg Reflector Grown on Sapphire. *Appl. Phys. Lett.* 2000, 76, 1804−1806.

(23) Waldrip, K. E.; Han, J.; Figiel, J. J.; Zhou, H.; Makarona, E.; Nurmikko, A. V. Stress Engineering during Metalorganic Chemical Vapor Deposition of AlGaN/GaN Distributed Bragg Reflectors. *Appl. Phys. Lett.* 2001, 78, 3205−3207.

(24) Yeh, P. S.; Yu, M.-C.; Lin, J.-H.; Huang, C.-C.; Liao, Y.-C.; Lin, D.-W.; Fan, J.-R.; Kuo, H.-C. GaN-Based Resonant-Cavity LEDs Featuring a Si-Diffusion-Defined Current Blocking Layer. *IEEE Photonics Technol. Lett.* 2014, 26, 2488−2491.

(25) Lin, C. F.; Yao, H. H.; Lu, J. W.; Hsieh, Y. L.; Kuo, H. C.; Wang, S. C. Characteristics of Stable Emission GaN-Based Resonant-Cavity Light-Emitting Diodes. *J. Cryst. Growth* 2004, 261, 359−363.

(26) Huang, G. S.; Lu, T. C.; Yao, H. H.; Kuo, H. C.; Wang, S. C.; Lin, C.-W.; Chang, L. Crack-Free GaN/AlN Distributed Bragg Reflectors Incorporated with GaN/AlN Superlattices Grown by Metalorganic Chemical Vapor Deposition. *Appl. Phys. Lett.* 2006, 88, No. 061904.

(27) Park, J.; Kang, J.-H.; Ryu, S.-W. High Diffuse Reflectivity of Nanoporous GaN Distributed Bragg Reflector Formed by Electro-chemical Etching. *Appl. Phys. Express* 2013, 6, No. 072201.

(28) Shiu, G.-Y.; Chen, K.-T.; Fan, F.-H.; Huang, K.-P.; Hsu, W.-J.; Dai, J.-J.; Lai, C.-F.; Lin, C.-F. InGaN Light-Emitting Diodes with an Embedded Nanoporous GaN Distributed Bragg Reflectors. *Sci. Rep.* 2016, 6, 29138.

(29) Zhang, C.; Park, S.-H.; Chen, D.; Lin, D.-W.; Xiong, W.; Kuo, H.-C.; Lin, C.-F.; Cao, H.; Han, J. Mesoporous GaN for Photonic Engineering Highly Reflective GaN Mirrors as an Example. *ACS Photonics* 2015, 2, 980−986.

(30) Hou, Y.; Syed, Z. A.; Jiu, L.; Bai, J.; Wang, T. Porosity-Enhanced Solar Powered Hydrogen Generation in GaN Photo-electrodes. *Appl. Phys. Lett.* 2017, 111, 203901.

(31) Day, J.; Li, J.; Lie, D. Y. C.; Bradford, C.; Lin, J. Y.; Jiang, H. X. III-Nitride Full-Scale High-Resolution Microdisplays. *Appl. Phys. Lett.* 2011, 99, No. 031116.

(32) Ju, Z. G.; Liu, W.; Zhang, Z.-H.; Tan, S. T.; Ji, Y.; Kyaw, Z. B.; Zhang, X. L.; Lu, S. P.; Zhang, Y. P.; Zhu, B. B.; Hasanov, N.; Sun, X. W.; Demir, H. V. Improved Hole Distribution in InGaN/GaN Light-Emitting Diodes with Graded Thickness Quantum Barriers. *Appl. Phys. Lett.* 2013, 102, 243504.

(33) Takeuchi, T.; Sota, S.; Katsuragawa, M.; Komori, M.; Takeuchi, H.; Amano, H.; Akasaki, I. Quantum-Confined Stark Effect Due to Piezoelectric Fields in GaInN Strained Quantum Wells. *Jpn. J. Appl. Phys.* 1997, 36, L382.

(34) Bai, J.; Xu, B.; Guzman, F. G.; Xing, K.; Gong, Y.; Hou, Y.; Wang, T. (11−22) Semi-Polar InGaN Emitters from Green to Amber on Overgrown GaN on Micro-Rod Templates. *Appl. Phys. Lett.* 2015, 107, 261103.